

# Structural and Immunochemical Analysis of the Lipopolysaccharide from *Acinetobacter lwoffii* F78 Located Outside *Chlamydiaceae* with a *Chlamydia*-Specific Lipopolysaccharide Epitope

Anna Hanuszkiewicz,<sup>[a]</sup> Göran Hübner,<sup>[b]</sup> Evgeny Vinogradov,<sup>[c]</sup> Buko Lindner,<sup>[b]</sup> Lore Brade,<sup>[d]</sup> Helmut Brade,<sup>[d]</sup> Jennifer Debarry,<sup>[e]</sup> Holger Heine,<sup>[e]</sup> and Otto Holst\*<sup>[a]</sup>

**Abstract:** Chemical analyses, NMR spectroscopy, and mass spectrometry were used to elucidate the structure of the rough lipopolysaccharide (LPS) isolated from *Acinetobacter lwoffii* F78. As a prominent feature, the core region of this LPS contained the disaccharide  $\alpha$ -Kdo-(2 $\rightarrow$ 8)- $\alpha$ -Kdo (Kdo=3-deoxy-d-d-manno-oct-2-ulopyranosonic acid), which so far has been identified only in chlamydial LPS. In serological investigations, the anti-chlamydial LPS monoclonal antibody S25-2, which is specific for the epitope  $\alpha$ -Kdo-(2 $\rightarrow$ 8)- $\alpha$ -Kdo, reacted with *A. lwoffii* F78 LPS. Thus, an LPS was identified outside *Chlamydiaceae* that contains a *Chlamydia*-specific LPS epitope in its core region.

**Keywords:** *Acinetobacter* • antibodies • lipopolysaccharides • mass spectrometry • NMR spectroscopy • structure elucidation

## Introduction

The genus *Acinetobacter* has gained in importance owing to the growing number of nosocomial infections caused by several of its species.<sup>[1–3]</sup> Mainly, clinical isolates belong to *A. baumannii*, however, the pathogenicity of some strains of *A.*

*lwoffii* and their resistance against antibiotics has been reported.<sup>[4–6]</sup> In general, *A. lwoffii* is an ubiquitous microorganism that can be isolated from soil, water, and food<sup>[7–9]</sup> as well as from human skin.<sup>[10]</sup> The strain investigated in this study, namely *A. lwoffii* F78, was isolated amongst other bacteria from a farm in Bavaria, Germany, in the course of an investigation on allergy-protective properties of bacterial species from farm environments.<sup>[11]</sup>

Bacteria belonging to the family *Chlamydiaceae* are human and animals pathogens possessing an unusual and characteristic life cycle, which sets them apart from other bacteria within their own order.<sup>[12]</sup> They are the causative agents of a number of diseases like pneumonia, trachoma (chronic infection of the eye, which in late stages leads to secondary blindness), sexually transmitted diseases (serovars D through K of *C. trachomatis* cause the most frequently diagnosed sexually transmitted infection), or atypical pneumonia caused by *Chlamydophila psittaci*, an avian pathogen, which might be transmitted to humans (psittacosis). These bacteria have also been connected to disorders like reactive arthritis or arteriosclerosis.<sup>[13,14]</sup>

Both, *Chlamydia* and *Acinetobacter* belong to the Gram-negative bacteria and thus possess lipopolysaccharide (LPS, endotoxin) as the main cell-wall constituent placed in the outer layer of the outer membrane.<sup>[15]</sup> In general, complete or smooth-form LPS contains a lipid portion (the lipid A), which, in the case of toxic LPS, represents its endotoxic

- [a] A. Hanuszkiewicz, Prof. O. Holst  
Division of Structural Biochemistry, Research Center Borstel  
Leibniz-Center for Medicine and Biosciences  
Parkallee 1–40, 23845 Borstel (Germany)  
Fax: (+49) 4537-188745  
E-mail: oholst@fz-borstel.de
- [b] G. Hübner, Dr. B. Lindner  
Division of Immunochemistry, Research Center Borstel  
Leibniz-Center for Medicine and Biosciences  
Parkallee 1–40, 23845 Borstel (Germany)
- [c] Dr. E. Vinogradov  
National Research Council, Institute for Biological Sciences  
Glycoanalysis, 100 Sussex Drive, Ottawa, ON, K1A 0R6 (Canada)
- [d] Dr. L. Brade, Prof. H. Brade  
Division of Medical and Biochemical Microbiology  
Research Center Borstel  
Leibniz-Center for Medicine and Biosciences  
Parkallee 1–40, 23845 Borstel (Germany)
- [e] Dr. J. Debarry, Dr. H. Heine  
Division of Innate Immunity, Research Center Borstel  
Leibniz-Center for Medicine and Biosciences  
Parkallee 1–40, 23845 Borstel (Germany)

Supporting information for this article is available on the WWW under <http://dx.doi.org/10.1002/chem.200800958>.

moiety. A polysaccharide, comprising a nonrepetitive oligosaccharide, the core region, and the O-specific polysaccharide (O-antigen), which is in most cases built up from repeating units consisting of various sugars, is linked to lipid A.<sup>[16]</sup> Rough(R)-form LPS, which may occur naturally or in laboratory strains, lacks the O-antigen. Such an LPS has been identified in *Chlamydiaceae*, which only possesses a short-core region that is exclusively furnished from 3-deoxy- $\alpha$ -D-manno-oct-2-ulopyranosonic acid (Kdo) residues. These residues build up the trisaccharide  $\alpha$ -Kdo-(2 $\rightarrow$ 8)- $\alpha$ -Kdo-(2 $\rightarrow$ 4)- $\alpha$ -Kdo, which represents the family-specific antigen.<sup>[17]</sup> Up to now, no other LPS containing this trisaccharide has been found outside *Chlamydiaceae*. In the case of the *Acinetobacter* species, the structures of many O-specific polysaccharides have been reported,<sup>[18–20]</sup> however, only a few core oligosaccharides are known to date.<sup>[21]</sup> We have now performed the structural and serological analyses of the (R)-form LPS from *A. lwoffii* F78 and identified in its core region the Kdo disaccharide  $\alpha$ -Kdo-(2 $\rightarrow$ 8)- $\alpha$ -Kdo, which represents part of the *Chlamydia*-LPS-specific epitope.<sup>[12,13]</sup> This molecule reacted with the *Chlamydia*-specific monoclonal antibody (mAb) S25–2.<sup>[22]</sup> Thus, besides the identification of a novel *Acinetobacter* LPS core structure, we report, for the first time, on the presence of the *Chlamydia*-LPS-specific epitope in an LPS of a bacterium outside *Chlamydiaceae* and prove its cross-reactivity with a monoclonal anti-chlamydial LPS antibody.

## Results

**Isolation and analyses of LPS:** The LPS was extracted from dry *A. lwoffii* F78 biomass to give a final yield of 1.0%. SDS-PAGE and Western blot (mAb A6)<sup>[23]</sup> analyses showed that the LPS was of the rough type, containing no O-antigen (Figure 1). The compositional as well as GC and GC-MS analyses proved the presence of GlcN, GalN, Glc, Kdo, phosphates, and dodecanoic (12:0) and (*R*)-3-hydroxy-dodecanoic [12:0(3-OH)] acid.

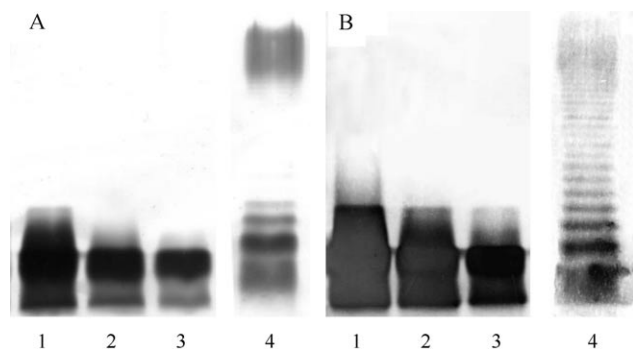


Figure 1. SDS/PAGE (A) and Western blot analysis with mAb A6 (B) of the LPS from *A. lwoffii* F78 (lane 1: 2.5  $\mu$ g; lane 2: 1  $\mu$ g; lane 3: 0.5  $\mu$ g; lane 4: whole-cell lysate from *S. enterica* sv. Typhimurium SL3770 as a control). The high molecular-weight banding pattern visible in *S. enterica* sv. Typhimurium SL3770 sample corresponded to the O-antigen, which was lacking in the LPS from *A. lwoffii* F78.

**Mass spectrometry:** Electrospray ionization Fourier-transform ion cyclotron resonance (ESI FT-ICR) mass spectra of the intact LPS showed the heterogeneity concerning both the core region and lipid A. In the core region, two core fractions were visible (Figure 2), one of which (fraction I)

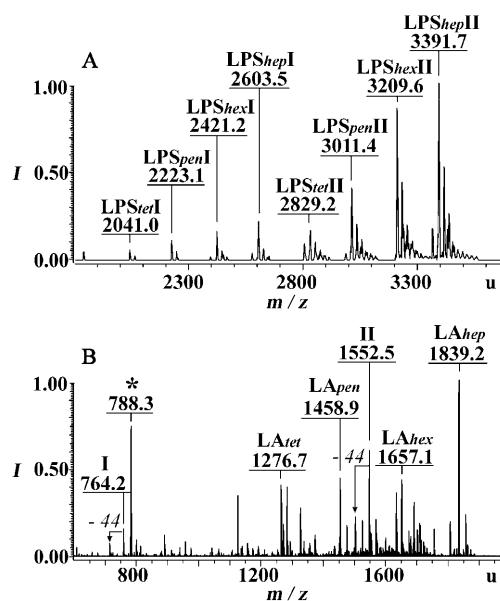


Figure 2. Negative-ion mode ESI FT-ICR MS of intact LPS molecule under soft ionization (A) and CSD conditions providing the fragmentation of the labile linkage between Kdo and lipid A (B). The difference of  $m/z$  44 in the case of the molecular ion of the complete core (II) at  $m/z$  1552.5 and at  $m/z$  764.2 (I) were owing to the decarboxylation of Kdo, which is characteristic of the cleavage between the Kdo and lipid A.<sup>[24]</sup> For assignment of the mass peak marked with an asterisk, see the text.

contained two Kdo and two Hex residues (Hex=hexose), and the other one (fraction II) contained an additional Kdo, one Hex, and two HexNAc residues. The molecular ion of the highest intensity (at  $m/z$  3391.7; Figure 2A) corresponded to the LPS with core fraction II bound to the hepta-acylated lipid A (LPS<sub>Shep</sub>II). The molecular ions at  $m/z$  3209.6, 3011.4, and 2829.2 corresponded to moieties comprising the LPS with core fraction II bound to hexa- (LPS<sub>hex</sub>II), penta- (LPS<sub>pen</sub>II) and tetra-acylated (LPS<sub>Stet</sub>II) lipid A, respectively. The molecular ion at  $m/z$  2603.5 was consistent with LPS containing only core fraction I linked to hepta-acylated lipid A (LPS<sub>Shep</sub>I), and ions at  $m/z$  2421.2, 2223.1, and 2041.0 corresponded to fraction I linked to hexa- (LPS<sub>hex</sub>I), penta- (LPS<sub>pen</sub>I), and tetra-acylated (LPS<sub>Stet</sub>I) lipid A, respectively. To confirm these results, the capillary skimmer dissociation (CSD) mass spectrum (Figure 2B) was generated, which led mainly to the cleavage of the labile linkage between Kdo and the lipid A. Beside molecular ions corresponding to all lipid-A moieties, also ions derived from the core fractions (I at  $m/z$  764.2 and II at  $m/z$  1552.5) were visible. The mass peak at  $m/z$  788.3 (Figure 2B, marked with asterisk) originated from the cleavage of the tetrasaccharide consisting of one Kdo, one Hex, and two HexNAc residues from the core fraction II owing to the high voltage applied.

In agreement with the analyses of the intact LPS, the mass spectrum of lipid A (see Figure 1 in the Supporting Information) showed four major pseudomolecular ions, all of them consistent with a HexNP disaccharide to which fatty acids were bound. The ion at  $m/z$  1276.7 corresponded to tetra-acylated lipid A (*LA<sub>tet</sub>*) containing one 12:0 and three 12:0(3-OH) fatty acid residues, and ions at  $m/z$  1458.9,  $m/z$  1657.1 and 1839.2 corresponded to penta- [*LA<sub>pen</sub>*; two 12:0 and three 12:0(3-OH)], hexa- [*LA<sub>hex</sub>*; two 12:0 and four 12:0(3-OH)], and hepta-acylated [*LA<sub>hep</sub>*; three 12:0 and four 12:0(3-OH)] lipid-A moieties, respectively. The mass spectrum of the *O*-deacylated lipid A (*LA<sub>di</sub>*) proved the amide-bound fatty acids to be 12:0(3-OH), molecular ion at  $m/z$  896.4; the ion at  $m/z$  816.4 corresponded to a molecule with one phosphate residue less (see Figure 1B in the Supporting Information). To elucidate the number and type of fatty acids linked to the reducing and non-reducing GlcN residues, MS-MS spectra in the positive-ion mode were recorded, which yielded an intensive B fragment of the non-reducing sugar of the lipid A (Figure 3A).<sup>[24]</sup> The mass of this fragment ( $m/z$  1001.6) indicated that four fatty acids were linked to the non-reducing GlcN in which two 12:0(3-OH) residues were linked to C2 (amide bound) and C3 (ester bound) of GlcN, both substituted at their 3-OH groups by 12:0. The fragment ions at  $m/z$  801.5 and  $m/z$  403.2 originated from further cleavage of 12:0 and [12:0(3-OH)-12:0], respectively. The fatty acid distribution on the distal GlcN was elucidated by MS-MS analysis in negative-ion mode, which revealed two different fatty acid distribution patterns, that is, one (*B<sub>1</sub>*; Figure 3) with a secondary 12:0 bound to ester-linked 12:0(3-OH) and the second (*B<sub>2</sub>*; Figure 3) with a secondary 12:0 linked to amide-bound 12:0(3-OH). The MS-MS spectra of hexa- and penta-acylated lipid A showed a very high heterogeneity in fatty acid distribution in both, Y and B fragments, which were similar to those published for *A. radioresistens*

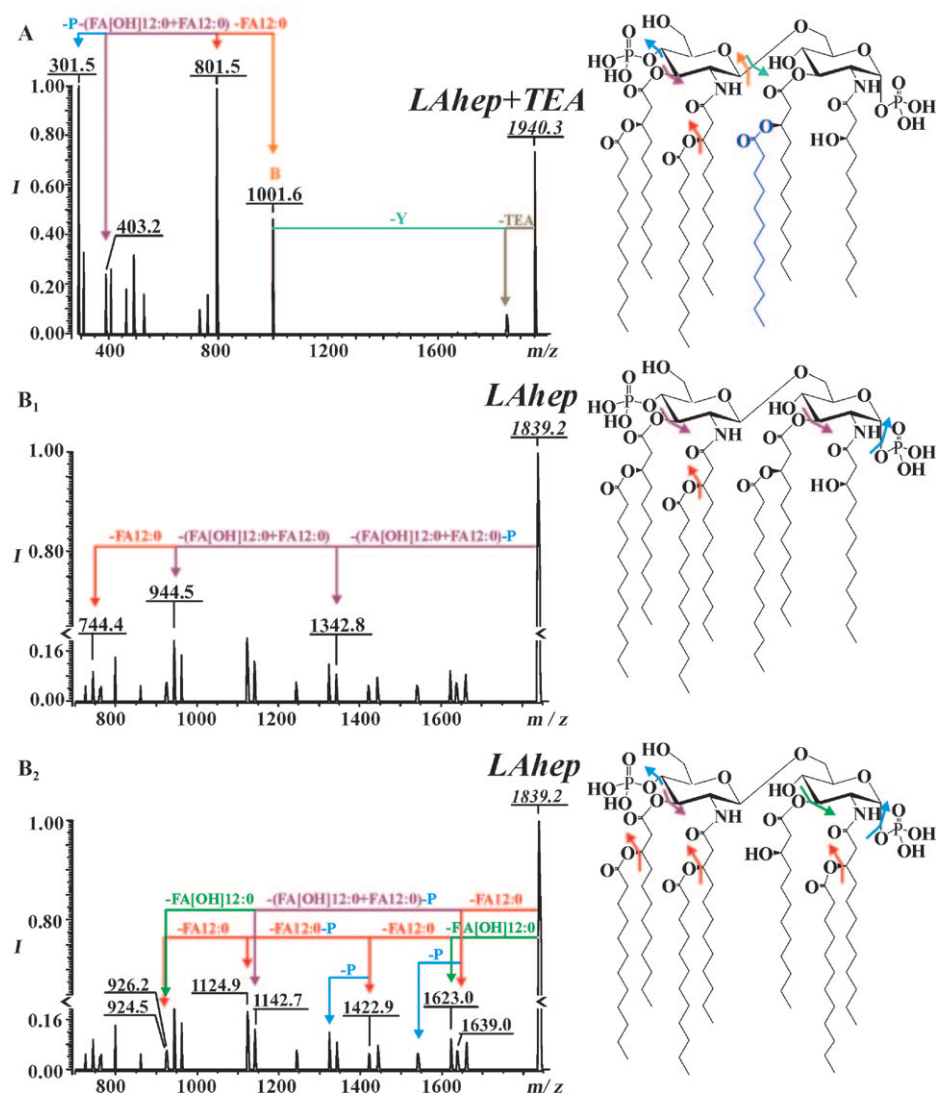
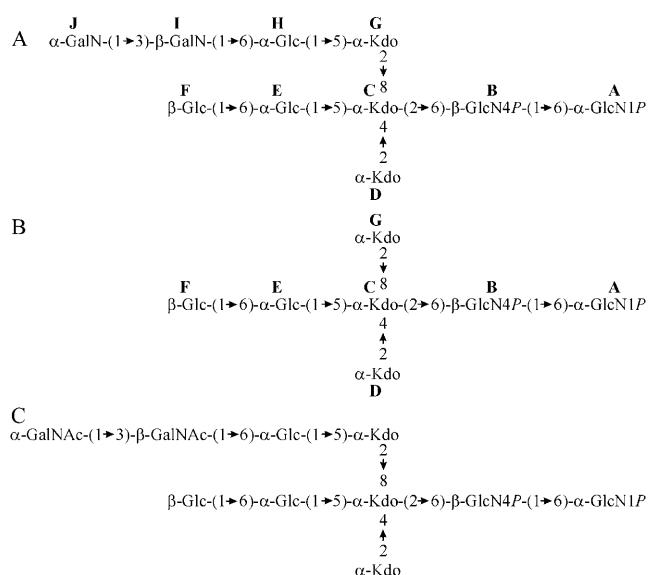


Figure 3. Positive- (A) and negative-ion mode (B) IRMPD ESI FT-ICR MS/MS spectra of hepta-acylated lipid A from LPS of *A. lwoffii* F78 (parent ion displayed in italic letters). The fragmentation pathway in spectrum A indicates the distribution of fatty acids on the non-reducing sugar (fragment B; structure on the right-hand side). The position of the third fatty acid (displayed in blue) on the reducing sugar (fragment Y) remained unclear in the positive-ion mode and was identified by the fragmentation pathways in the negative-ion-mode spectrum (presented twice in *B<sub>1</sub>* and *B<sub>2</sub>* for increased clarity), which showed two possibilities (structures shown on the right-hand side).

*S13*.<sup>[25,26]</sup> The tetra-acylated molecular species was not analyzed by MS-MS owing to its very low intensity.

**Structural analyses of the oligosaccharides:** For the complete structural determination by NMR spectroscopy, only the two major fractions (of six; see Table 1 in the Supporting Information) obtained by high-performance anion-exchange chromatography (HPAEC) were used, namely oligosaccharides **1** and **2** (4 mg each), which represents the complete carbohydrate backbone of the LPS. The only difference between them was the presence of an *N*-acetyl group in residue **I** (see Scheme 1A) in oligosaccharide **2**, thus, only the complete data obtained for oligosaccharide **1** is presented. The <sup>1</sup>H NMR assignments were based on correlation spec-



Scheme 1. The structures of oligosaccharide **1** (A), oligosaccharide **6** (B), and of the carbohydrate backbone of the LPS from *A. lwoffii* F78 (C). All sugars are D-configured pyranoses.

troscopy ( $^1\text{H}, ^1\text{H}$  COSY), total correlation spectroscopy (TOCSY), rotating nuclear Overhauser effect spectroscopy (ROESY), and  $^1\text{H}, ^{13}\text{C}$  heteronuclear multiple quantum coherence (HMQC) as well as the  $^{13}\text{C}$  assignments on  $^1\text{H}, ^{13}\text{C}$  heteronuclear multiple bond correlation (HMBC) and HMQC spectra (Table 1). The positions of the phosphate groups were determined by applying  $^1\text{H}, ^{31}\text{P}$  HMQC experiments. The anomeric region of the  $^1\text{H}$  NMR spectrum (Figure 4) contained seven signals, which, on the basis of coupling constants analysis, belonged to four  $\alpha$ - (**A**, **J**, **E**, **H**) and three  $\beta$ -configured (**B**, **I**, **F**) residues. Two sugars pos-

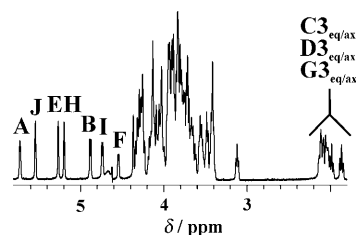


Figure 4.  $^1\text{H}$  NMR spectrum of oligosaccharide **1** (recorded at 42 °C).

Table 1. Chemical shifts of protons and carbon atoms (in ppm) of oligosaccharide **1**.<sup>[a]</sup>

	H1/C1	H2/C2	H3/C3	H4/C4	H5/C5	H6a/C6	H6b/C6	H7/C7	H8a/C8	H8b/C8
<b>A</b> $\alpha$ -GlcN1P	5.72 3.18 <sup>[b]</sup> 91.73	3.47 55.22	3.94 70.23	3.70 70.27	4.16 73.18	3.80 <i>70.44</i>	4.31			
<b>B</b> $\beta$ -GlcN4P	4.87 8.54 <sup>[b]</sup> 100.17	3.12 56.35	3.90 72.58	3.83 75.03	3.78 74.67	3.47 <i>63.19</i>	3.74			
<b>C</b> $\alpha$ -Kdo	174.73	100.70	2.02/2.11 35.35	3.98 72.48	4.28 75.12	3.71 73.4		4.12 69.0	3.64 64.5	3.92
<b>D</b> $\alpha$ -Kdo	175.20	103.24	1.84/2.01 35.35	3.87 66.48	4.02 68.10	3.74 72.5		4.04 71.6	3.81 61.7	3.81
<b>E</b> $\alpha$ -Glc	5.26 <1 <sup>[b]</sup> 100.51	3.55 72.92	3.84 72.53	3.69 68.88	4.11 71.92	3.88 <i>66.06</i>	4.05			
<b>F</b> $\beta$ -Glc	4.52 7.32 <sup>[b]</sup> 101.82	3.52 75.59	3.62 76.14	3.39 70.39	3.4 76.3	3.71 61.71	3.88			
<b>G</b> $\alpha$ -Kdo	175.62	100.01	1.96/2.08 36.76	4.24 66.48	4.12 76.69	3.91 72.8		4.24 69.1	3.80 61.5	3.86
<b>H</b> $\alpha$ -Glc	5.17 <1 <sup>[b]</sup> 100.96	3.56 72.88	3.82 73.43	3.41 70.84	4.29 71.69	3.87 <i>70.24</i>	4.25			
<b>I</b> $\beta$ -GalN	4.72 8.54 <sup>[b]</sup> 100.78	3.42 52.61	4.10 74.45	4.36 63.78	3.74 75.86	3.81 61.85	3.85			
<b>J</b> $\alpha$ -GalN	5.53 <1 <sup>[b]</sup> 92.36	3.64 51.23	4.23 67.07	4.07 68.6	4.02 73.0	3.79 63.52	3.95			

[a] Shifts shown in italics indicate the binding positions. [b]  $J_{1,2}$  coupling constant (in Hz).

sessed the *galacto* configuration (residues **I** and **J**), all other sugars were *gluco* configured. All residues were present in the pyranose form. Residues **A**, **B**, **I**, and **J** carried an amino group at C2 ( $^{13}\text{C}$  signals of C2 at  $\delta=55.22$ , 56.35, 52.61, and 51.23 ppm, respectively). The  $^1\text{H}$ ,  $^{31}\text{P}$  HMQC spectrum contained a  $^{31}\text{P}$  signal at  $\delta=0.52$  ppm, which correlated with that of proton A1 and a  $^{31}\text{P}$  signal at  $\delta=0.82$  ppm with that of proton B4. Among inter-residual NOE connectivities (ROESY, Table 2) was a strong NOE connectivity from J1

Table 2. NOE connectivities observed in the ROESY spectrum of oligosaccharide **1**.

From proton	To proton
B1	A6a
E1	C5
F1	E6a/6b
H1	G5
I1	H6a/6b
J1	I3; I4

to I4, which could be explained by a specific conformation of the oligosaccharide and was also indicated by the strong upfield shift of carbon J1 (92.36 ppm), however, this was not proven. In the case of the Kdo residues, it was possible to assign the attachment sites for residue **D** (long-range correlation between D2 and C4) and for residue **C** (long-range correlation between C2 and B6b) by the HMBC experiment. Yet, the correlation between G2 and C8a and/or C8b was not visible in any of the spectra. The substitution of C8 was deduced, based on its downfield shift (64.50 ppm) in comparison to unsubstituted D8 and G8 (61.70 ppm and 61.50 ppm, respectively). The HMBC experiment proved the sequence of other sugar residues showing the long-range H-C correlations, namely between proton B1 and carbon A6, proton E1 and carbon C5, proton F1 and carbon E6, proton H1 and carbon G5, proton I1 and carbon H6, and proton J1 and carbon I3. Furthermore, the substitution pattern of the sugar residues was confirmed by methylation analysis of the LPS. Hydrolysis of the methylated sample with 2M trifluoroacetic acid allowed identification of terminal and 6-substituted hexoses. Additional hydrolysis in 4M trifluoroacetic acid proved the presence of terminal, 3-, and 6-substituted HexN in the  $\text{CHCl}_3/\text{MeOH}$  fraction (see the Experimental Section) and terminal, 5-substituted, 4,5-substituted (residue **C** in the molecule containing only core fraction **I**), and 4,5,8-substituted Kdo residues in the diethyl ether fraction. The ESI FT-ICR mass spectrum (Figure 2) of oligosaccharide **1** confirmed its structure. The absolute configuration of Glc, GalN, and GlcN were assigned on the basis of L- or D-configured standards. All these sugars in oligosaccharide **1** were D-configured. Thus, the structure of oligosaccharide **1** was as depicted in Scheme 1A.

In the LPS, the amino groups of the GalN residues are substituted by acetyl groups (Scheme 1), as deduced from the fragmentation patterns of the core regions in the ESI FT-ICR mass spectra and the presence of one acetyl group

on the C2 amino group of residue **I** in oligosaccharide **2** (data not shown).

The oligosaccharides **3–6** isolated by HPAEC were of too low intensity to record the complete NMR spectra, however,  $^1\text{H}$  NMR, TOCSY, COSY, and ESI MS analyses and comparison with data from oligosaccharides **1** and **2** allowed us to assign their structure (Figure 3 and Figure 4 in the Supporting Information). Oligosaccharide **3** comprised the core fraction II lacking one GalN residue ( $m/z$  1807.5), oligosaccharide **4** contained only core fraction I ( $m/z$  1264.3), oligosaccharide **5** consisted of the core fraction II without both GalN residues ( $m/z$  1646.4), and oligosaccharide **6** contained core fraction II without the hexoses side chain on Kdo G ( $m/z$  1484.4).

**Serology:** The TLC immuno-overlay experiments showed the reaction of one band of the *A. lwoffii* F78 LPS with mAb S25–2, but not with mAb S25–23 (Figure 5). Both

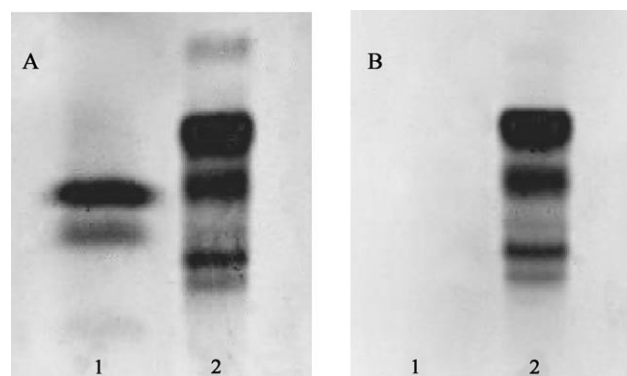


Figure 5. Immunostained TLC with mAbs S25–2 (A), specific for Kdo-(2→8)-Kdo and S25–23 (B), specific for Kdo-(2→8)-Kdo-(2→4)-Kdo; (lane 1: 5 µg LPS from *A. lwoffii* F78; lane 2: 0.5 µg LPS from *E. coli* F515–207).

mAbs represent anti-*Chlamydia* LPS-specific antibodies, the former of which is able to bind to the  $\alpha$ -Kdo-(2→8)- $\alpha$ -Kdo moiety, whereas the latter requires  $\alpha$ -Kdo-(2→8)- $\alpha$ -Kdo-(2→4)- $\alpha$ -Kdo trisaccharide present in all chlamydial LPS.<sup>[22]</sup> The fact that bigger amounts of *A. lwoffii* F78 LPS (5 µg) were required in comparison with the control LPS of recombinant *E. coli* F515–207 (0.5 µg)<sup>[27]</sup> indicated that the S25–2-reactive molecular species represented a minor fraction of the total LPS preparation. Thus, we deduced that it was not the entire LPS which reacted with the antibody, but a smaller derivative that contained a truncated core lacking the GalNAc and Glc residues bound to Kdo (Scheme 1B). This molecule exposed the  $\alpha$ -Kdo-(2→8)- $\alpha$ -Kdo epitope that could react with mAb S25–2. It was identified in ESI FT-ICR mass spectra of the entire LPS (data not shown) and its carbohydrate backbone was isolated by HPAEC (oligosaccharide **6**), however, the small amounts of this compound did not allow a complete NMR analysis. The  $^1\text{H}$  NMR spectrum (see Figure 4C in the Supporting Information) showed the presence of residues **A–G**, and COSY

and ROESY experiments confirmed the same linkages of these residues as in oligosaccharide **1**. The ESI FT-ICR mass spectrum was consistent with NMR data (Figure 4C in the Supporting Information).

## Discussion

It is known for *Acinetobacter* LPS that the O-antigen, although present in many cases, cannot be visualized by silver-stained SDS/PAGE and might only be revealed by a Western blot with antibodies specific to the O-chain or lipid A.<sup>[28]</sup> In the case of *A. lwoffii* F78, we used mAb A6, which recognizes the bisphosphorylated lipid A disaccharide,<sup>[23]</sup> and could make it possible to visualize the O-antigen on a Western blot. However, there was no O-antigen visible, proving the presence of a rough-type LPS in *A. lwoffii* F78. Until now, only one fully characterized *Acinetobacter* lipid A has been published, namely the one isolated from LPS of *A. radioresistens* S13,<sup>[25]</sup> the other reports present data on the identified fatty acids derived from lipid A moieties.<sup>[29–32]</sup> In all cases, the presence of 12:0 and 12:0(3-OH), which were characteristically the only fatty acids present in *A. lwoffii* F78 lipid A. However, in contrast with the previously described molecules of lipid A, *A. lwoffii* F78 LPS did neither contain 12:0(2-OH) nor 14:0(3-OH). Still, it possessed a similar heterogeneity as reported for the lipid A of LPS from *A. radioresistens* S13<sup>[25,26]</sup> with respect to both distribution and character of fatty acids. This held true for all four molecular species, that is, hepta-, hexa-, penta-, and tetraacylated lipid A.

To date, only a few *Acinetobacter* core oligosaccharides have been structurally characterized.<sup>[32]</sup> All of these lack heptoses, as is the case for *A. lwoffii* F78 LPS. However, previously characterized in *Acinetobacter* LPS D-glycero-D-talo-oct-2-octulopyranosonic acid (of LPS from *Acinetobacter* strain ATCC 17905 and *A. haemolyticus* ATCC 17906), was not found in *A. lwoffii* F78. Instead, it contains a 4,5,8-substituted Kdo residue that, up to now, was described only in LPS of *Proteus mirabilis*, *P. penneri*, and in *Serratia marcescens* 111R.<sup>[33–35]</sup> Yet, in those LPSs, it was  $\beta$ -L-Arap4N that substituted Kdo at position 8, whereas in *A. lwoffii* F78 LPS another Kdo residue was linked to this position, thus furnishing a  $\alpha$ -Kdo-(2 $\rightarrow$ 8)- $\alpha$ -Kdo disaccharide moiety that had been identified only in *Chlamydia* LPS before.<sup>[31,36]</sup> An 8-substituted Kdo residue was already found in LPS from the *A. baumannii* strain NCTC 10303,<sup>[31]</sup> however, the substituting element was a tetrasaccharide built of  $\alpha$ -(1 $\rightarrow$ 3)-linked L-Rhap units. In addition to the structural similarity between the LPS of *A. lwoffii* F78 and *Chlamydiae*, one fraction of the *A. lwoffii* F78 LPS, which was separated by TLC, could be visualized by immuno-overlay (Figure 5) with *Chlamydiaceae*-specific mAb S25–2.<sup>[22]</sup>

In general, *Chlamydia* and *Chlamydophila* comprise several species that are pathogenic in humans and animals. Chlamydial LPS contains the family-specific epitope  $\alpha$ -Kdo-(2 $\rightarrow$ 8)- $\alpha$ -Kdo-(2 $\rightarrow$ 4)- $\alpha$ -Kdo,<sup>[12,17]</sup> against which a number of

mAbs have been raised and described.<sup>[13,37,38]</sup> Some of them require the complete trisaccharide sequence, whereas others also bind to the partial disaccharide structure  $\alpha$ -Kdo-(2 $\rightarrow$ 8)- $\alpha$ -Kdo. Among the latter is mAb S25–2, whose structure has been determined by X-ray crystallography to be unligated and in complex with numerous natural and synthetic ligands.<sup>[17,39]</sup> This mAb together with those recognizing the trisaccharide epitope are specific for the whole family and are therefore used in clinical microbiological laboratories to identify *Chlamydiae* isolated from patient samples. On the other hand, the epitope is highly immunogenic, giving rise to the production of antibodies after experimental immunization or after natural infection. Thus, the cross-reaction described herein is relevant for clinical diagnosis of chlamydial infections as it may result in false-positive interpretations. It is therefore strongly advised for the detection of *Chlamydiae* in patient samples in microbiological diagnostic laboratories to apply monospecific antibodies that react with the trisaccharide  $\alpha$ -Kdo-(2 $\rightarrow$ 8)- $\alpha$ -Kdo-(2 $\rightarrow$ 4)- $\alpha$ -Kdo only, like mAb S25–23.<sup>[22]</sup> Although the cross-reactivity between *Acinetobacter* and *Chlamydia* had been reported for the first time more than 50 years ago and has been confirmed by several groups including ours,<sup>[40,41]</sup> the molecular basis of this phenomenon has not yet been clarified. The cross-reactivity in *Chlamydia*-specific clinical tests has, however, only been reported a few times,<sup>[41–43]</sup> which seriously hinders immuno-tests for fast and reliable detection of chlamydial infection. The LPS of one of the cross-reacting *Acinetobacter* strains was already intensively investigated,<sup>[40,44,45]</sup> yet no similarity to chlamydial LPS epitopes was found in its structure. Herein, we could not yet determine the exact chemical structure of the fraction that gives rise to the positive reaction in TLC immuno-overlay (Figure 5), however, oligosaccharide **6** was found to be an inhibitor of mAb S25–2 in an inhibition ELISA experiment although at 50-times higher molar concentrations as the free  $\alpha$ -Kdo-(2 $\rightarrow$ 8)- $\alpha$ -Kdo disaccharide (data not shown). However, the small amounts of oligosaccharide **6** did not allow its conjugation to protein, which would thereby enable more-detailed binding studies. We are currently trying to generate defined mutants of *A. lwoffii* F78 that synthesize oligosaccharide **6** in higher yields.

## Conclusion

Herein, immunochemical examinations of the rough-type LPS of *A. lwoffii* F78 were performed by means of NMR spectroscopy, mass spectrometry, and chemical analyses. The LPS isolate was heterogeneous in both the core oligosaccharide and lipid A. The branched core region contained a  $\alpha$ -Kdo-(2 $\rightarrow$ 8)- $\alpha$ -Kdo moiety that has been known before only as a part of the *Chlamydia*-LPS-specific epitope. The LPS from *A. lwoffii* F78 reacted with the *Chlamydia*-LPS-specific mAb S25–2. Such cross-reactivity between *Chlamydia* and *Acinetobacter* had been described earlier; however, the character of responsible antigen epitope(s) remained unclear. The present work indicates a molecular basis for this

cross-reactivity. *Acinetobacter* and *Chlamydia* are both important human pathogens and a correct serological differentiation between these bacteria is of great importance in clinical diagnostics. As the reaction of *A. lwoffii* F78 LPS with mAb S25–2 required relatively high concentrations of the substrate (10 times more than control LPS), further studies are necessary to demonstrate which of the LPS species is/are responsible for this reactivity.

## Experimental Section

**Bacterial strain and LPS isolation:** Strain *A. lwoffii* F78 was isolated from a farm in Bavaria, Germany, and grown in Super Broth [SB; 30 g tryptone, 20 g yeast extract, 4-morpholine propane sulfonic acid (MOPS; 10 g)], supplemented with of 2 M glucose (10 mL<sup>-1</sup> SB) at 30°C. A 10-L culture was maintained in four 2.5-L flasks and bacteria were centrifuged after 48 h, washed with ethanol (4°C, 16 h), then twice with acetone (4°C, 2 h), and once with diethyl ether, and dried. The LPS was extracted with hot phenol/water,<sup>[46]</sup> and the water phase containing the LPS was further purified by enzymatic treatment (RNase A, Sigma-Aldrich, USA; DNase I, Roche, Germany; Proteinase K, Roche, Germany). The nucleases were applied at 37°C in a buffer solution consisting of 0.01 M MgCl<sub>2</sub>, 0.05 M NaCl, and 0.1 M Tris-HCl [pH 7.5; Tris = tris(hydroxymethyl)amino-methane] for 12 h, and Proteinase K was subsequently utilized at 56°C for 1 h. Then, the LPS was ultracentrifuged (105,000×g, 4°C, 24 h) and re-extracted with PCP III (phenol/chloroform/light petroleum 1:1:1, by volume).<sup>[44]</sup>

**Analyses:** The LPS was subjected to SDS-PAGE (12% acrylamide in the separating gel, silver stain) and Western blot by utilizing anti-lipid A mAb A6 as previously described.<sup>[23]</sup> The quantification of sugars and fatty acids by GC, and of HexN, Kdo, and organic-bound phosphate, and the determination of the absolute configuration of the sugars and hydroxy fatty acids were performed as described.<sup>[47]</sup> For methylation analysis, 0.5 mg of LPS was dephosphorylated with 48% aqueous HF (4°C, 16 h). Methylation was performed with MeI in DMSO at 22°C,<sup>[48]</sup> and the methylated product was extracted with CHCl<sub>3</sub>, evaporated to dryness under nitrogen, and methylated again. The sample was hydrolyzed with 2 M trifluoroacetic acid at 100°C for 2 h and then reduced with NaBD<sub>4</sub> in water (22°C, 16 h). After terminating the reaction with 8 M HCl and evaporation, the sample was reduced again with NaBD<sub>4</sub> in MeOH/H<sub>2</sub>O (1:4, by vol., 4°C, 16 h), then acetylated and analyzed by GC–MS. Next, the sample was hydrolyzed with 4 M trifluoroacetic acid (100°C, 4 h), reduced with NaBD<sub>4</sub> in MeOH/H<sub>2</sub>O (1:4, by vol., 4°C, 16 h), acetylated, and analyzed by GC–MS. Finally, the sample was evaporated, dissolved in diethyl ether and passed through a column of silica gel placed in a Pasteur pipette. The silica gel was rinsed twice with diethyl ether to elute all neutral sugars followed by CHCl<sub>3</sub>/MeOH (19:1, by vol.) to obtain the amino sugars fraction. Both, diethyl ether and CHCl<sub>3</sub>/MeOH fractions were evaporated and analyzed by GC–MS.

**Isolation of oligosaccharides:** To obtain the core oligosaccharides in pure form for NMR analysis, the LPS (45 mg) was O-deacylated by mild hydrazinolysis, subsequently N-deacylated by hot KOH, and the oligosaccharides were isolated by HPAEC as described,<sup>[47]</sup> but with the modification that the column was eluted with a linear gradient of 1–30% 1 M sodium acetate (pH 6) over 2 h.

**Preparation of lipid A and O-deacylated lipid A:** The LPS (5 mg) was hydrolyzed in acetate buffer solution (pH 4.4, 1 mL, 100°C, 2 h). The released lipid A was centrifuged (10,000×g, 4°C, 15 min), resuspended in H<sub>2</sub>O, and extracted four times with CHCl<sub>3</sub>/MeOH (4:1, v/v). The lipid A and the O-deacylated (by hydrazinolysis)<sup>[47]</sup> lipid A were analyzed by ESI FT-ICR MS.

**Mass spectrometry:** ESI FT-ICR MS analyses were performed on a 7 Tesla Apex II (Bruker Daltonics, USA). For the negative-ion mode, the samples were solved in a water/2-propanol/triethylamine mixture (50:50:0.001, v/v/v), and for the positive-ion mode in 5 mM ammonium

acetate/2-propanol/triethylamine mixture (50:50:0.05, v/v/v). The samples were sprayed at a flow rate of 2 μL min<sup>-1</sup>. Capillary entrance voltage was set to 3.8 kV, and dry gas temperature to 150°C. CSD was induced in negative-ion mode by increasing the capillary exit voltage from –100 V to –350 V. The spectra, which showed several charge states for each component, were charge deconvoluted, and mass numbers given refer to the monoisotopic molecular masses. Infrared multiphoton dissociation (IRMPD) of isolated parent ions was performed in positive-ion mode with a 35 W, 10.6 μm CO<sub>2</sub> laser (Synrad, Mukilteo, WA). The unfocused laser beam was directed through the center of the ICR cell and fragment ions were detected after a delay of 0.5 ms. The duration of laser irradiation was adapted for each sample to generate optimal fragmentation and varied between 10–80 ms.<sup>[24]</sup>

**NMR spectroscopy:** 1D and 2D <sup>1</sup>H,<sup>1</sup>H COSY, TOCSY, ROESY, <sup>1</sup>H,<sup>13</sup>C HMBC and HMQC, and <sup>1</sup>H,<sup>31</sup>P HMQC NMR spectra were recorded either at 42°C or 27°C on solutions of D<sub>2</sub>O with a Bruker AMX 600 spectrometer applying standard Bruker software. The spectral width for <sup>1</sup>H, <sup>13</sup>C correlations was 6009 Hz in the F2 dimension and 31,694 Hz in the F1 dimension. A mixing time of 250 ms was used for the ROESY experiments. The spin-lock field strength corresponded to a 90° pulse with 35 μs and the mixing time of 100 ms was used for TOCSY. The resonances were measured relative to internal acetone ( $\delta_{\text{H}}=2.225$  ppm;  $\delta_{\text{C}}=31.45$  ppm) and to external 85% phosphoric acid ( $\delta_{\text{P}}=0$  ppm).

**Serology:** Lipopolysaccharide samples were separated by TLC<sup>[17]</sup> and then stained with two *Chlamydia*-specific antibodies, namely S25–2 and S25–23;<sup>[22]</sup> LPS from *Escherichia coli* F515–207 was used as a positive control.<sup>[27]</sup> Staining was performed with a fluorescent secondary antibody and analyzed in Li-Cor's Odyssey Infrared Imaging System.

## Acknowledgements

We thank Hermann Moll, Heiko Käbner, Regina Engel, Irina von Cube, Ute Agge, and Andreas Beyer for their technical assistance and Dr. Zbigniew Kaczyński for discussion. This work was financially supported by Deutsche Forschungsgemeinschaft (project SFB-TR22 A02 and Z01). Parts of this work were presented at the Baltic Meeting on Microbial Carbohydrates 2006, October 4–8, Rostock, Germany, the Joint Meeting of SLB/IEHS 2006, November 9–11, San Antonio, TX, USA, the 55th ASMS Conference on Mass Spectrometry and Allied Topics, June 3–7, Indianapolis, IN, USA, and the 14th European Carbohydrate Symposium, September 2–7, 2007, Lübeck, Germany.

- [1] E. Bergogne-Berezin, K. J. Towner, *Clin. Microbiol. Rev.* **1996**, *9*, 148–165.
- [2] S. Misbah, H. Hassan, M. Y. Yusof, Y. A. Hanifah, S. AbuBakar, *Singapore Med. J.* **2005**, *46*, 461–464.
- [3] L. Dijkshoorn, A. Nemeec, H. Seifert, *Nat. Rev. Microbiol.* **2007**, *5*, 939–951.
- [4] T. Mori, T. Nakazato, R. Yamazaki, Y. Ikeda, S. Okamoto, *Intern. Med.* **2006**, *45*, 803–804.
- [5] M. Perilli, A. Felici, A. Oratore, G. Cornaglia, G. Bonfiglio, G. M. Rossolini, G. Amicosante, *Antimicrob. Agents Chemother.* **1996**, *40*, 715–719.
- [6] Y. Zavros, G. Rieder, A. Ferguson, J. L. Merchant, *Infect. Immun.* **2000**, *70*, 2630–2639.
- [7] P. Baumann, *J. Bacteriol.* **1968**, *96*, 39–42.
- [8] M. Gennari, M. Parini, D. Volpon, M. Serio, *Int. J. Food Microbiol.* **1992**, *15*, 61–75.
- [9] M. Gennari, P. Lombardi, *Zentralbl. Bakteriologie* **1993**, *279*, 553–564.
- [10] H. Seifert, L. Dijkshoorn, P. Gerner-Smidt, N. Pelzer, I. Tjernberg, M. Vaneechoutte, *J. Clin. Microbiol.* **1997**, *35*, 2819–2825.
- [11] J. Debarry, H. Garn, A. Hanuszkiewicz, N. Dickgreber, N. Blümer, E. von Mutius, A. Bufe, S. Gatermann, H. Renz, O. Holst, H. Heine, *J. Allergy Clin. Immunol.* **2007**, *119*, 1514–1521.

- [12] H. Brade in *Endotoxin in health and disease* (Eds.: H. Brade, S. M. Opal, S. N. Vogel, D. C. Morrison), Marcel Dekker, New York, Basel, **1999**, p. 229–256.
- [13] H. Brade, W. Brabetz, L. Brade, O. Holst, S. Löbau, M. Lucakova, U. Mamat, A. Różalski, K. Zych, P. Kosma, *J. Endotoxin Res.* **1997**, *4*, 67–84.
- [14] M. Chmiela, M. Kowalewicz-Kulbat, A. Miszczak, M. Wiśniewska, T. Rechciński, K. Kołodziej, J. Kasprzak, T. Wadstrom, W. Rudnicka, *FEMS Immunol. Med. Microbiol.* **2003**, *36*, 187–192.
- [15] O. Holst, S. Müller-Loennies in *Comprehensive Glycoscience*, (Eds.: J. P. Kamerling, G.-J. Boons, Y. C. Lee, A. Suzuki, N. Taniguchi, A. G. J. Voragen), Elsevier, Oxford, UK, **2007**, p. 123–178.
- [16] C. Alexander, E. T. Rietschel, *J. Endotoxin Res.* **2001**, *7*, 167–202.
- [17] S. Müller-Loennies, S. Gronow, L. Brade, R. MacKenzie, P. Kosma, H. Brade, *Glycobiology* **2006**, *16*, 184–196; and references therein.
- [18] L. Galbraith, J. L. Sharples, S. G. Wilkinson, *Carbohydr. Res.* **1999**, *319*, 204–208.
- [19] R. Pantophlet, A. Nemeč, L. Brade, H. Brade, L. Dijkshoorn, *J. Clin. Microbiol.* **2001**, *39*, 2576–2580.
- [20] R. Pantophlet, L. Brade, H. Brade, *Clin. Diagn. Lab. Immunol.* **2001**, *8*, 825–827.
- [21] E. V. Vinogradov, L. Brade, H. Brade, O. Holst, *Carbohydr. Res.* **2003**, *338*, 2751–2756.
- [22] Y. Fu, M. Baumann, P. Kosma, L. Brade, H. Brade, *Infect. Immun.* **1992**, *60*, 1314–1321.
- [23] R. Pantophlet, L. Brade, H. Brade, *J. Endotoxin Res.* **1997**, *4*, 89–95.
- [24] A. N. Kondakova, E. V. Vinogradov, Y. A. Knirel, B. Lindner, *Rapid Commun. Mass Spectrom.* **2005**, *19*, 2343–2349.
- [25] S. Leone, L. Sturiale, E. Pessione, R. Mazzoli, C. Giunta, R. Lanzetta, D. Garozzo, A. Molinaro, M. Parrilli, *J. Lipid Res.* **2007**, *48*, 1045–1051.
- [26] S. Leone, A. Molinaro, E. Pessione, R. Mazzoli, C. Giunta, L. Sturiale, D. Garozzo, R. Lanzetta, M. Parrilli, *Carbohydr. Res.* **2006**, *341*, 582–590.
- [27] O. Holst, W. Broer, J. E. Thomas-Oates, U. Mamat, H. Brade, *Eur. J. Biochem.* **1993**, *214*, 703–710.
- [28] R. Pantophlet, In *Acinetobacter, molecular microbiology*, (Ed.: U. Gerischer), Caister Academic Press, Norfolk, UK, **2008**, p. 61–98.
- [29] E. V. Vinogradov, S. Müller-Loennies, B. O. Petersen, S. Meshkov, J. E. Thomas-Oates, O. Holst, H. Brade, *Eur. J. Biochem.* **1997**, *247*, 82–90.
- [30] E. V. Vinogradov, K. Bock, B. O. Petersen, O. Holst, H. Brade, *Eur. J. Biochem.* **1997**, *243*, 122–127.
- [31] E. V. Vinogradov, B. O. Petersen, J. E. Thomas-Oates, J. Duus, H. Brade, O. Holst, *J. Biol. Chem.* **1998**, *273*, 28122–28131.
- [32] E. V. Vinogradov, J. O. Duus, H. Brade, O. Holst, *Eur. J. Biochem.* **2002**, *269*, 422–430, and references therein.
- [33] O. Holst in *Endotoxin in health and disease* (Eds.: H. Brade, S. M. Opal, S. N. Vogel, D. C. Morrison), Marcel Dekker, New York, Basel, **1999**, p. 115–154.
- [34] O. Holst, *Trends Glycosci. Glycotechnol.* **2002**, *14*, 87–103.
- [35] O. Holst, *FEMS Microbiol. Lett.* **2007**, *271*, 3–11.
- [36] H. Brade, L. Brade, F. E. Nano, *Proc. Natl. Acad. Sci. USA* **1987**, *84*, 2508–2512.
- [37] L. Brade, O. Holst, P. Kosma, Y. X. Zhang, H. Paulsen, R. Krause, H. Brade, *Infect. Immun.* **1990**, *58*, 205–213.
- [38] H. D. Caldwell, P. J. Hitchcock, *Infect. Immun.* **1984**, *44*, 306–314.
- [39] C. L. Brooks, S. Müller-Loennies, L. Brade, P. Kosma, T. Hiram, C. R. MacKenzie, H. Brade, S. V. Evans, *J. Mol. Biol.* **2008**, *377*, 450–468.
- [40] H. Brade, H. Brunner, *J. Clin. Microbiol.* **1979**, *10*, 819–822.
- [41] M. Nurminen, E. Wahlstrom, M. Kleemola, M. Leinonen, P. Saikku, P. H. Mäkelä, *Infect. Immun.* **1984**, *44*, 609–613.
- [42] I. Haralambieva, I. Iankov, D. Petrov, R. Ivanova, B. Kamarinchev, I. Mitov, *Diagn. Microbiol. Infect. Dis.* **2001**, *41*, 99–106.
- [43] D. Taylor-Robinson, B. J. Thomas, M. F. Osborn, *J. Clin. Pathol.* **1987**, *40*, 194–199.
- [44] H. Brade, C. Galanos, *Eur. J. Biochem.* **1982**, *122*, 233–237.
- [45] H. Brade, A. Tacke, R. Christian, *Carbohydr. Res.* **1987**, *167*, 295–300.
- [46] O. Westphal, K. Jann, *Methods Carbohydr. Chem.* **1965**, *5*, 83–91.
- [47] C. Oertelt, B. Lindner, M. Skurnik, O. Holst, *Eur. J. Biochem.* **2001**, *268*, 554–564.
- [48] S. Hakomori, *J. Biochem.* **1964**, *55*, 205–208.

Received: May 20, 2008  
Published online: October 10, 2008